

The Reflection Phase Grating Diffusor: Design Theory and Application*

PETER D'ANTONIO AND JOHN H. KONNERT

RPG Diffusor Systems, Inc., Largo, MD 20772, USA

The far-field diffraction theory of the Schroeder reflection phase grating diffusor, which provides broad-bandwidth wide-angle coverage, is reviewed. Design parameters are discussed, and theoretical diffraction patterns are presented for a quadratic-residue and a primitive-root example. The diffraction patterns are obtained using a new reflection phase grating program, which was developed to facilitate the design and evaluation of these acoustical diffusors. Experimental energy-time curves are presented and discussed for two models. A few recording studio applications are mentioned, and a recent installation is pictured. Observations in recording control rooms suggest that the reflection phase grating diffusor helps maintain the stereo perspective across the width of the mixing console and adds the sweetening of a concert hall to a treated room.

0 INTRODUCTION

Many new and ingenious advances in architectural acoustics have been made in the last decade at the University of Göttingen, Germany, which hold promise for major improvements in the acoustics of sound recording and monitoring environments. Schroeder and his collaborators [1]–[6] have shown that, in addition to reverberation and spectral balance, lateral sound diffusion is a significant parameter which decreases interaural coherence (the similarity of sound reaching each ear) and increases listener preference in concert halls. To increase the amount of lateral diffusion, Schroeder developed a highly diffusing surface, which acts like a reflection phase grating and provides back-scattering over a wide range of angles and over a broad bandwidth. With regard to reverberation, Schroeder and Hackman [7] and Gilbert [8] have recently shown that accurate values for reverberation time can indeed be calculated using integral equations for the spatial and temporal energy balance. The calculations reveal the inaccuracies of the classical formulas, which do not include room shape, absorber location, and the state of diffusion.

In an effort to stimulate the application and evaluation of the reflection phase grating diffusor, in acoustic

spaces and critical listening environments as one would have in a recording studio and control room, we would like to:

- 1) Review the far-field Fraunhofer diffraction theory
- 2) Describe the necessary design parameters
- 3) Present a quadratic-residue (QR) and a primitive-root (PR) diffusor model example
- 4) Present calculated far-field diffraction patterns obtained with a new reflection phase grating computer-aided design and evaluation program—RPG¹
- 5) Contrast the dynamic interference effects from a QR, a PR, and a cylindrical diffusor as a function of the frequency and duration of the incident sound
- 6) Present and explain experimental energy-time measurements on a QR and a PR diffusor model
- 7) Discuss a few applications, installations, and observations.

1 THEORY

Many approaches have been used to improve the diffusion of sound in critical acoustic environments. Room dimensions have been optimized, ceilings have been inclined, and walls splayed. Room surfaces have been covered with geometrically irregular shapes, po-

* Presented at the 74th Convention of the Audio Engineering Society, New York, 1983 October 8–12; revised 1984 January 31.

¹ RPG is a registered trademark of RPG Diffusor Systems, Inc.

lycylindrical columns, and/or alternating absorbing and reflecting panels. All methods have attempted to distribute the incident waves by scattering them into many wavelets having equal energy over a wide angular range. In addition, it was hoped that this spatial distribution occurred over a broad range of frequencies, thereby making the acoustical characteristics of the room more uniform. The Schroeder diffusor can accomplish all these goals in a predictable fashion. The one-dimensional diffusor consists of a periodic grouping of an array of slots or wells of equal width, but different depths, separated by thin and rigid walls. In the two-dimensional diffusor the different-depth wells and their rigid dividing well walls form a lattice or grid pattern. Two space-filling examples are an orthogonal array of contiguous square or rectangular wells and a hexagonal network of hexagonal wells. The well depths are determined by mathematical sequences which have the critical property that the Fourier transform of the exponentiated sequence values has constant magnitude. The QR sequence satisfies this requirement exactly at the design frequency f_0 , or the lowest frequency at which there is efficient diffusion, and multiples thereof. At nonintegral multiples of f_0 the transform is approximately constant. The PR sequence provides approximate, but satisfactorily constant magnitude over the scattering bandwidth. A scaled cross section of two periods of a one-dimensional QR diffusor is shown in Fig. 1.

A QR sequence is generated by n^2 modulo N , which is the least non-negative remainder, modulo an odd prime number N , where n ranges between zero and infinity. The sequence values for $N = 17$ are shown in Table 1. It can be seen that the sequence has mirror symmetry at $n = 0$ and between $n = (N \pm 1)/2$ and is periodic, with N wells per period. The PR sequence is generated from the function g^n modulo N . Here again N is an odd prime and g is the least primitive root of N . The PR sequence values for $N = 17$ and $g = 3$ are also listed in Table 1. Notice that there are only $N - 1$ sequence values and no mirror symmetry. The numbers from 1 to 17 are permuted, but occur only once in the sequence.

The actual depth of the n^{th} well is given by

$$d_n = \frac{S_n \lambda_0}{2N} \quad (1)$$

where $\lambda_0(c/f_0)$ is the design wavelength and c is the velocity of sound. The well depths vary from zero to approximately $\lambda_0/2$, with an average value of $\lambda_0/4$. S_n represents either the QR or the PR sequence values. Since the sequences are periodic, the scattered wavelets have definite phase relationships among them. This is due to the fact that each wavelet involved in the scattering process experiences a different path length. The path-length differences introduce phase differences, which cause interference effects. In certain directions, constructive interference takes place, and the scattering phenomenon known as diffraction occurs. The diffracted

waves are composed of a large number of scattered wavelets mutually reinforcing one another. To determine the diffraction angles, α_d , shown in Fig. 1, at which the scattering intensity is a maximum, we can make use of the construction shown in Fig. 2. Here we show corresponding points in six periods with a repeat distance NW and ignore for the moment the wells of different depths within these periods. Consider incident wavelets AB and EG , which make an angle α_i with the surface normal. Incident wavelet EG travels a distance FG farther than AB before reaching the surface, and the scattered wavelet BD travels a distance BC farther than GH after leaving the surface. The difference in path lengths between wavelets $ABCD$ and $EFGH$ is $BC - FG$. This difference must equal a whole number of wavelengths if constructive interference is to occur at α_d . Therefore $BC - FG$ must equal $m\lambda$, where λ is the wavelength of the incident sound and m is a positive or negative integer. From Fig. 2 it can be seen that $BC = NW \sin \alpha_d$ and $FG = -NW \sin \alpha_i$.

$$m\lambda = NW(\sin \alpha_d + \sin \alpha_i) \quad (2a)$$

$$\sin \alpha_d = \frac{m\lambda}{NW} - \sin \alpha_i \quad (2b)$$

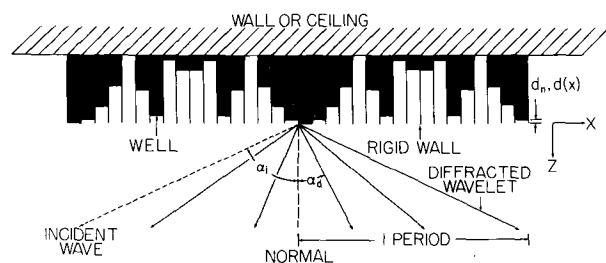


Fig. 1. Scaled cross section of a one-dimensional QR diffusor described in Schroeder [5], consisting of two periods, with 17 wells per period ($N = 17$). The width W of each of the wells, which are separated by thin and rigid walls, is equal to $0.137\lambda_0$, where λ_0 is the design wavelength. d_n is the depth of the n^{th} well, and $d(x)$ is the depth at the lateral position x . A wavefront (dashed line) making an angle of incidence α_i of -65° with the surface normal and five diffracted wavelets (solid lines) occurring at $\alpha_d = -54.2^\circ, -22.4^\circ, 2.7^\circ, 28.5^\circ$, and 65° are shown.

Table 1. One-dimensional QR and PR sequence values for $N = 17$.

n	$n^2_{\text{mod } 17}$	$3^n_{\text{mod } 17}$
0	0	—
1	1	3
2	4	9
3	9	10
4	16	13
5	8	5
6	2	15
7	15	11
8	13	16
9	13	14
10	15	8
11	2	7
12	8	4
13	16	12
14	9	2
15	4	6
16	1	1

For a given angle of incidence α_i , α_d depends only on the repeat distance NW , the value of the wavelength λ , and the value of m , which may take on any value consistent with the magnitude of $\sin \alpha_d$, not exceeding unity. For an incident wavefront making an angle of incidence of -65° with the surface normal, the diffraction angles calculated from Eq. (2b) for $N = 17$, $\lambda = \lambda_0$, and $W = 0.137\lambda_0$, are $\alpha_d = -54.2^\circ, -22.4^\circ, 2.7^\circ, 28.5^\circ,$ and 65° , as shown in Fig. 1.

The intensities of these diffracted waves are also determined by phase relations among all wavelets scattered by the wells. The phase shift of a wavelet, arriving perpendicular to the surface, traveling down and back up the n^{th} well, is $-2\pi(2d_n)/\lambda$. The reflection factor $r(x)$ is given by

$$r(x) = \exp\left[-2\pi i \frac{2d(x)}{\lambda}\right] \quad (3)$$

where $i = \sqrt{-1}$ and $d(x)$ is the depth at the lateral position x , shown in Fig. 1. $d(x)$ is equal to d_n for all values of x within the n^{th} well and changes abruptly when the next well is encountered. Using the Fraunhofer far-field theory, the scattering amplitude $a(s)$ in all the scattered directions, indicated by the scattering vector s , is given by the Fourier transform of the reflection factor, at a reference plane $z = 0$ in Fig. 1, over the total length L of the diffusor:

$$a(s) = 1/L \int_0^L \exp\left[-4\pi i \frac{d(x)}{\lambda}\right] \exp[isx] dx \quad (4a)$$

$$= 1/L \int_0^L \exp\left[isx - 4\pi i \frac{d(x)}{\lambda}\right] dx \quad (4b)$$

where the magnitude of the scattering vector s is related to the angle of incidence and the angle of diffraction by

$$s = 2\pi \frac{\sin \alpha_d}{\lambda} - 2\pi \frac{\sin \alpha_i}{\lambda} \quad (5)$$

If we approximate the integral in Eq. (4b) with a sum, replace dx with Δx , and make use of the relation $\exp(i\phi) = \cos \phi - i \sin \phi$, where $\phi = sx - 4\pi d(x)/\lambda$

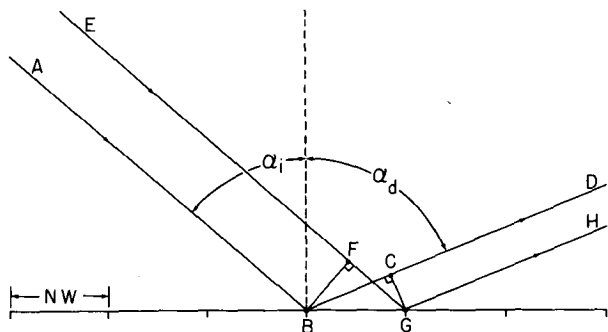


Fig. 2. Construction showing incident (A and E) and diffracted (D and H) wavelets from the surface of a periodic reflection phase grating with a repeat distance NW . The angle of incidence is α_i and the angle of diffraction α_d .

λ , we obtain the following expression:

$$|a(s)| = 1/NX \left\{ \left[\sum_{k=1}^{NX} \cos\left(sx - 4\pi \frac{d_k(x)}{\lambda}\right) \right]^2 + \left[\sum_{k=1}^{NX} \sin\left(sx - 4\pi \frac{d_k(x)}{\lambda}\right) \right]^2 \right\}^{1/2} \quad (6)$$

$\Delta x = W/NS$ and $L = NP NW$, where NS is the number of samples of the depth per well and NP is the number of periods. $\Delta x/L = 1/NX$, where NX is the total number of depth sample points.

In physical realizations of these diffusors, the number of periods is finite, that is, one or more, and the scattering occurs slightly below and above the diffraction directions, producing broad lobes, as seen in Fig. 3(a). Fig. 3(b) shows the diffraction pattern for the

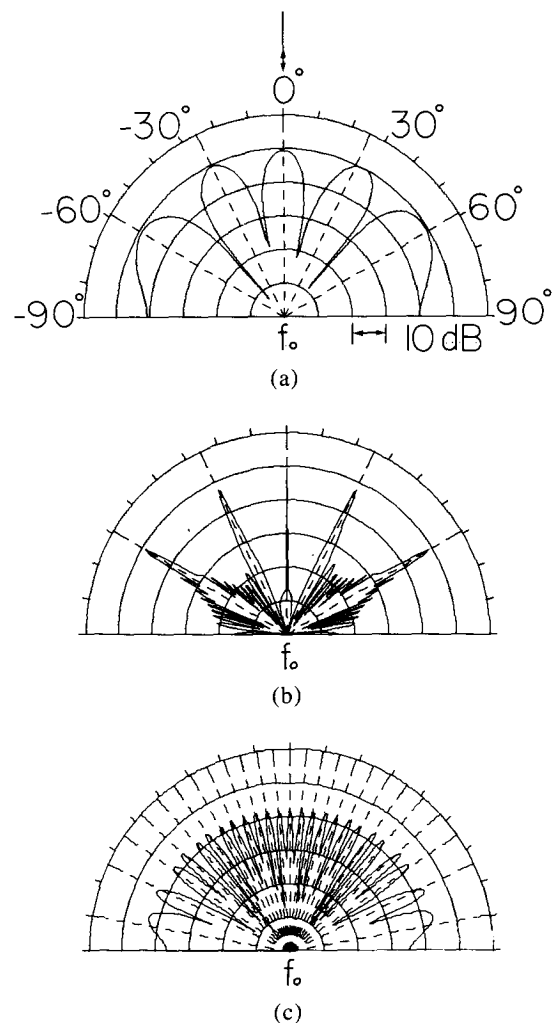


Fig. 3. (a) Scattering intensity pattern for the QR diffusor shown in Fig. 1. The diffraction directions are represented as dashed lines and the scattering from the finite diffusor occurs over broad lobes. The maximum intensity, for $\lambda = \lambda_0$ and $\alpha_i = 0^\circ$, has been normalized to 50 dB. (b) The number of periods has been increased from 2 to 25, concentrating energy in the diffraction directions. (c) The number of wells per period has been increased from 17 to 89, thereby increasing the number of lobes by a factor of 5. Arrows indicate incident and specular reflection directions.

diffusor described in Fig. 1, with 25 periods instead of 2. Increasing the number of periods concentrates the energy in the diffraction directions and sharpens the lobes. Since the integral in Eq. (4b) and the sums in Eq. (6) are carried out over the actual length of the diffusor, this broadening can be modeled. Fig. 3(c) shows the diffraction pattern for the diffusor in Fig. 1, with 89 wells per period instead of 17. The number of lobes and the diffusion have increased by a factor of 5.

More accurate theories, which require extensive computational power, have been presented by Schroeder et al. [3], [9], Berkhout et al. [10], and Strube [11]–[13]. The far-field theory is presented here as an introduction to the properties of the reflection phase grating and because Eqs. (1)–(6) can easily be programmed on a personal computer. In actual designs, where the listening position is close to the diffusors, as in recording control rooms, the diffraction patterns in the near field, as well as the limiting far field, must be evaluated. In the RPG program these calculations are implemented so that the optimum period length, maximum depth, well width, grouping or arrangement of periodic units, and placement in a room can be determined. Trial models can be conveniently designed and evaluated for custom installations.

2 DESIGN PARAMETERS

Specification of the bandwidth and the maximum order m_{\max} at the design frequency is sufficient to determine the remaining design parameters— W , N , and the depth sequence d_n . The bandwidth is defined as the difference between the design frequency f_0 and the maximum frequency f_{\max} which is limited by the well width, such that

$$f_{\max} = \frac{c}{2W} \quad (7)$$

Behavior above f_{\max} and below f_0 tends to be specular, but it can be optimized using the RPG program.

The well-wall separators, which are necessary for good diffusion, particularly for obliquely incident sound, are required to be thin and rigid so that, in effect, the wells provide a physical step function. In actual models the well walls have a finite width T , which can be taken into account by replacing W with $W + T$:

$$f_{\max} = \frac{c}{2(W + T)} \quad (8)$$

T should be kept as small as possible to minimize specular losses. Using Eq. (2), including the wall thickness T , at $f_0(c/\lambda_0)$, with $\alpha_i = 0^\circ$ and $|\sin \alpha_d| = 1$, we obtain an expression which specifies N , the number of wells per period,

$$N = \frac{m_{\max}c}{f_0(W + T)} \quad (9)$$

When $\alpha_i = 0^\circ$, we have $(2m_{\max} + 1)$ lobes between $\alpha_d = \pm 90^\circ$. For good diffusion at f_0 , we can set $m_{\max} = 2$, yielding five diffraction lobes. The larger m_{\max} , the greater the diffusion. For $\alpha_i \neq 0^\circ$ we do not have an equal number of lobes on either side of α_i , since for some, $|\sin \alpha_d| > 1$. Another useful relation can be obtained by substituting Eq. (8) into Eq. (9):

$$N = \frac{2m_{\max}f_{\max}}{f_0} \quad (10)$$

It must be kept in mind that N is required to be an odd prime. The value of N calculated from Eqs. (9) and (10) will generally have to be adjusted to the next closest larger prime so that none of the $(2m_{\max} + 1)$ lobes at f_0 is evanescent ($|\sin \alpha_d| > 1$).

Having specified f_0 and determined N , we can now calculate the depth sequence:

$$d_n = \frac{S_n c}{2N f_0} \quad (11)$$

3 EXAMPLE

We can use Eqs. (7)–(11) to design a QR diffusor with the following parameters: $f_0 = 1130$ Hz, $f_{\max} = 13\,560$ Hz, $m_{\max} = 2$, $T = 0$, and $c = 13\,560$ in/s. Substitution in Eqs. (8) and (10) yields $W = 0.5$ in (12.7 mm) and $N = 48$, respectively. The closest odd prime greater than 48 is 53. The sequence $n^2_{\text{mod } 53}$ need only be calculated for $0 \leq n = 26$, since there is mirror symmetry between $n = 26$ and $n = 27$, and the sequence is periodic in N . The values for the well number, n , $n^2_{\text{mod } 53}$, and d_n , are listed in Table 2. The diffraction patterns, calculated with the RPG program, are shown in Fig. 4 at $\frac{3}{4}f_0$, f_0 , $4f_0$, $8f_0$, and $12f_0$. All intensity patterns are given in decibels and are normalized, such that the maximum intensity $|a(s)|^2_{\max}$, at $f = f_0$, $\alpha_i = 0^\circ$, and $T = 0$ is 50 dB:

$$I(s) = 10 \log_{10} \left[\frac{|a(s)|^2 10^5}{|a(s)|^2_{\max}} \right] \quad [\text{dB}] \quad (12)$$

The far-field theory predicts good wide-angle diffusion over the entire frequency range. For $\alpha_i = -60^\circ$, Fig. 5 shows good diffusion up to $8f_0$.

The introduction of well walls of finite thickness, $T = 0.063$ in (1.6 mm) has several consequences:

1) The period changes from 26.5 in (637 mm) to 29.8 in (757 mm), changing the diffraction angles from 0° , $\pm 26.9^\circ$, and $\pm 64.9^\circ$ to 0° , $\pm 23.7^\circ$, and $\pm 53.5^\circ$.

2) f_{\max} is reduced from 13 560 to 12 040 Hz.

3) The intensities calculated using Eq. (6) are changed because $d(x)$ no longer changes value when a new well is reached. Instead, $T/\Delta x$ zero-depth samples are encountered, causing a perturbation in the depth sequence. In the diffraction pattern calculations, eight well-depth samples ($W/\Delta x$) and one well-wall zero-depth sample ($T/\Delta x$) per well, are used in the $d(x)$ array.

The intensity shown in Fig. 6(a) is peaked 5 dB in

the forward direction, and less scattering is obtained in the vicinity of $\alpha_d = \pm 90^\circ$. If T is decreased to 0.016 in (0.4 mm), perturbations in the depth sequence are reduced, and a diffraction pattern as shown in Fig. 6(b), more closely resembling $T = 0$, is obtained.

The same parameters as those used in the QR diffusor example can be used to create a PR diffusor. Substitution in Eqs. (8) and (10) yields $W = 0.5$ in (12.7 mm) and $N - 1 = 48$. In a PR sequence there are $N - 1$ sequence values and wells, instead of N , as was the case for a QR sequence. The closest odd prime, however, is again 53, as we had in the QR diffusor example. The sequence values can now be calculated from $g_{\text{mod } 53}^n$, where $g = 2$. The values of the well number, n , $2^n_{\text{mod } 53}$, and d_n , are listed in Table 2. The diffraction patterns, obtained

Table 2. Sequence values and well depths for a QR and a PR diffusor with $N = 53$ and $f_0 = 1130$ Hz.

n	$n^2_{\text{mod } 53}$	Well Depth d (in)	$2^n_{\text{mod } 53}$	Well Depth d (in)
0	0	0.000	—	—
1	1	0.113	2	0.226
2	4	0.453	4	0.453
3	9	1.019	8	0.906
4	16	1.811	16	1.811
5	25	2.830	32	3.623
6	36	4.075	11	1.245
7	49	5.547	22	2.491
8	11	1.245	44	4.981
9	28	3.170	35	3.962
10	47	5.321	17	1.925
11	15	1.698	34	3.849
12	38	4.302	15	1.698
13	10	1.132	30	3.396
14	37	4.189	7	0.792
15	13	1.472	14	1.585
16	44	4.981	28	3.170
17	24	2.717	3	0.340
18	6	0.679	6	0.679
19	43	4.868	12	1.358
20	29	3.283	24	2.717
21	17	1.925	48	5.434
22	7	0.792	43	4.868
23	52	5.887	33	3.736
24	46	5.208	13	1.472
25	42	4.755	26	2.943
26	40	4.528	52	5.887
27	40	4.528	51	5.774
28	42	4.755	49	5.547
29	46	5.208	45	5.094
30	52	5.887	37	4.189
31	7	0.792	21	2.377
32	17	1.925	42	4.755
33	29	3.283	31	3.509
34	43	4.868	9	1.019
35	6	0.679	18	2.038
36	24	2.717	36	4.075
37	44	4.981	19	2.151
38	13	1.472	38	4.302
39	37	4.189	23	2.604
40	10	1.132	46	5.208
41	38	4.302	39	4.415
42	15	1.698	25	2.830
43	47	5.321	50	5.660
44	28	3.170	47	5.321
45	11	1.245	41	4.642
46	49	5.547	29	3.283
47	36	4.075	5	0.566
48	25	2.830	10	1.132
49	16	1.811	20	2.264
50	9	1.019	40	4.528
51	4	0.453	27	3.057
52	1	0.113	1	0.113

using the RPG program, are shown in Fig. 7 for $\frac{3}{4}f_0$, f_0 , $4f_0$, $8f_0$, and $12f_0$. Notice the pronounced dip in the specular direction. This occurs for the PR sequence because the arguments for the sine and cosine terms in Eq. (6) are uniformly sampled over the range of zero to 2π . As a result the calculated amplitude is zero for the design frequency and multiples thereof. This is not the case, however, for $f < f_0$, and we note the

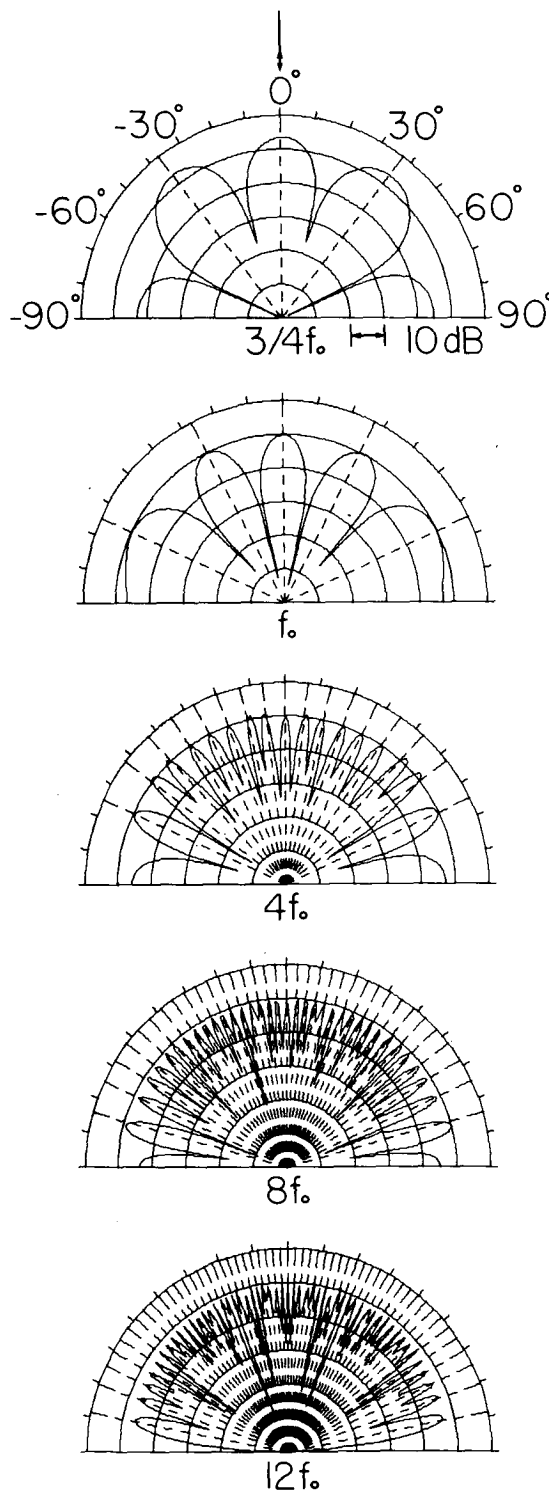


Fig. 4. Diffraction patterns at $\frac{3}{4}f_0$, f_0 , $4f_0$, $8f_0$ and $12f_0$, from two periods of a QR diffusor with parameters: $N = 53$, $W = 0.5$ in (12.7 mm), $T = 0$, $f_0 = 1130$ Hz, and $\alpha_i = 0^\circ$. Arrows indicate incident and specular reflection directions.

large specular reflection for $\frac{3}{4}f_0$. It can be seen that the diffusion is excellent over the design bandwidth.

As a comparison, the intensity scattered from a cylindrical surface, with a cord length of 12 in (0.3 m) and a height of 3 in (0.076 m), is approximately 12 dB down at $12f_0$, yielding a limited bandwidth.

4 APPLICATION

Schroeder originally developed the reflection phase grating diffusors to enhance the acoustics of concert

halls and auditoriums, but they can be used anywhere broad-bandwidth wide-angle diffusion is required. The reflection phase grating diffusors can be optimally placed on the walls and ceiling of a recording studio to tailor the overall diffusion and reverberation characteristics of the room; or they can be applied, in the near field, to specific areas reserved for recording particular instruments, such as strings, horns, or acoustic piano. These diffusors can also be used to improve the acoustics of a small isolation room, drum booth or mobile studio by increasing the density of reflected wavelets, thereby adding ambience and body to the sound. Acoustic reverberation chambers can be optimized to provide uniform diffusion, having a natural buildup and decay.

As a result of observations using time-delay spectrometry, developed by Heyser [14]–[16], Davis and Davis [17] proposed a new live-end–dead-end (LEDE)² concept for the control of acoustic and psychoacoustic parameters in recording control rooms. In these rooms the front surface surrounding the monitor loudspeakers is as absorptive as possible and the rear surface is hard and diffusive. The reflection phase grating diffusor is ideally suited to provide the diffuse sound field required in the rear, live end of the LEDE room. RPG models were first used in a recording environment at Under-

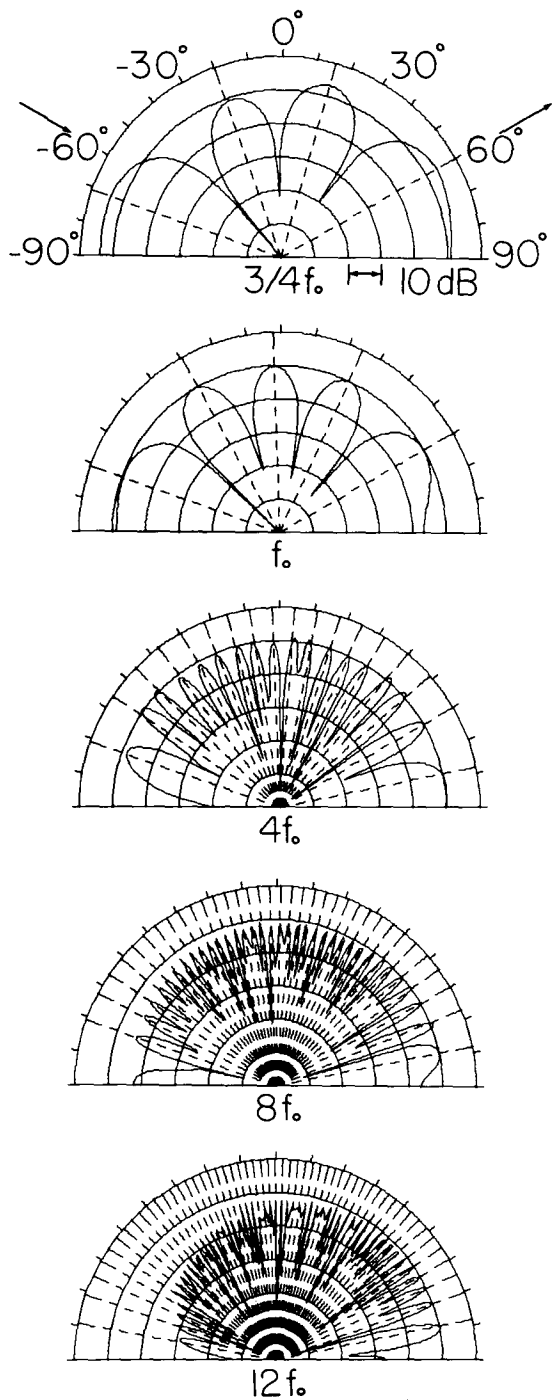


Fig. 5. Diffraction patterns at $\frac{3}{4}f_0$, f_0 , $4f_0$, $8f_0$, and $12f_0$ from two periods of a QR diffusor with parameters: $N = 53$, $W = 0.5$ in (12.7 mm), $T = 0$, $f_0 = 1130$ Hz, and $\alpha_i = -60^\circ$. Arrows indicate incident and specular reflection directions.

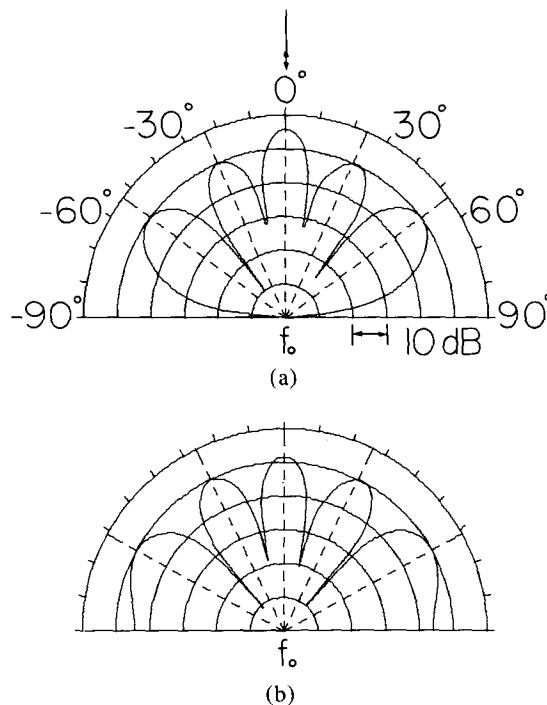


Fig. 6. (a) Diffraction pattern at $f = f_0$ from two periods of a QR diffusor with parameters: $N = 53$, $W = 0.5$ in (12.7 mm), $T = 0.063$ in (1.6 mm), $f_0 = 1130$ Hz, and $\alpha_i = 0^\circ$. The finite well walls have perturbed the QR depth sequence and affected the diffraction pattern. (b) Decreasing the well walls to 0.016 in (0.4 mm) decreases these perturbations and produces a pattern similar to Fig. 4. Arrows indicate incident and specular reflection directions.

² LEDE is a registered trademark of Synergetic Audio Concepts.

ground Sound Recording Studio in Largo, Maryland, where they were applied both in the studio and to the rear, live wall of the control room. A QR model containing two periods, with 23 wells per period (RPG-QR23), and a PR model with 22 wells per period (RPG-PR22) are shown in Fig. 8. The models have a design bandwidth of over a decade. Fairly narrow and deep

wells are necessary to provide coherent scattering over the broad range of frequencies that is required for recording studio applications. The deep wells permit low-frequency diffusion and the narrow wells allow coherent scattering of frequencies with wavelengths greater than twice the well widths. In these broad-bandwidth designs care should be taken to minimize resonance and transmission losses, especially at low frequencies. A recent installation of an RPG diffusor, with a bandwidth of over four octaves, at Acorn Sound Recorders in Hen-

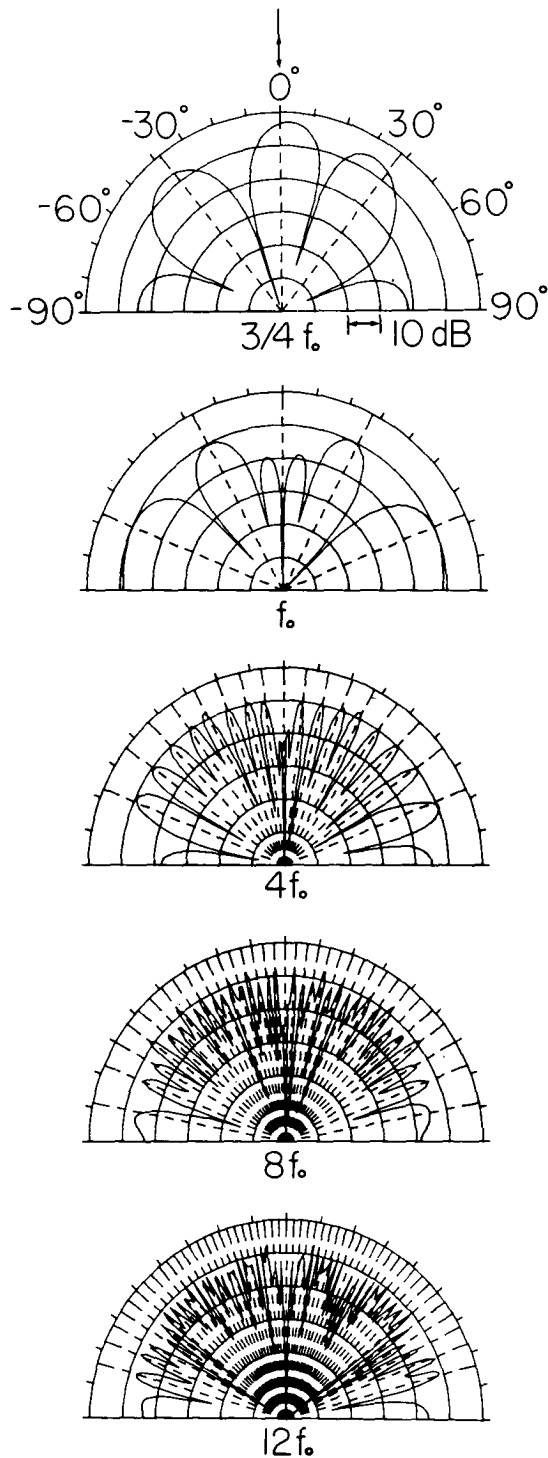


Fig. 7. Diffraction patterns at $\frac{3}{4}f_0$, f_0 , $4f_0$, $8f_0$, and $12f_0$ from two periods of a PR diffusor with parameters: $N = 53$, $W = 0.5$ in (12.7 mm), $T = 0$, $f_0 = 1130$ Hz, and $\alpha_i = 0^\circ$. Arrows indicate incident and specular reflection directions. Notice the pronounced specular dip at f_0 and integer multiples thereof. This occurs because the PR sequence affords a uniform sampling of the phase, in the range of zero to 2π , resulting in a zero amplitude.

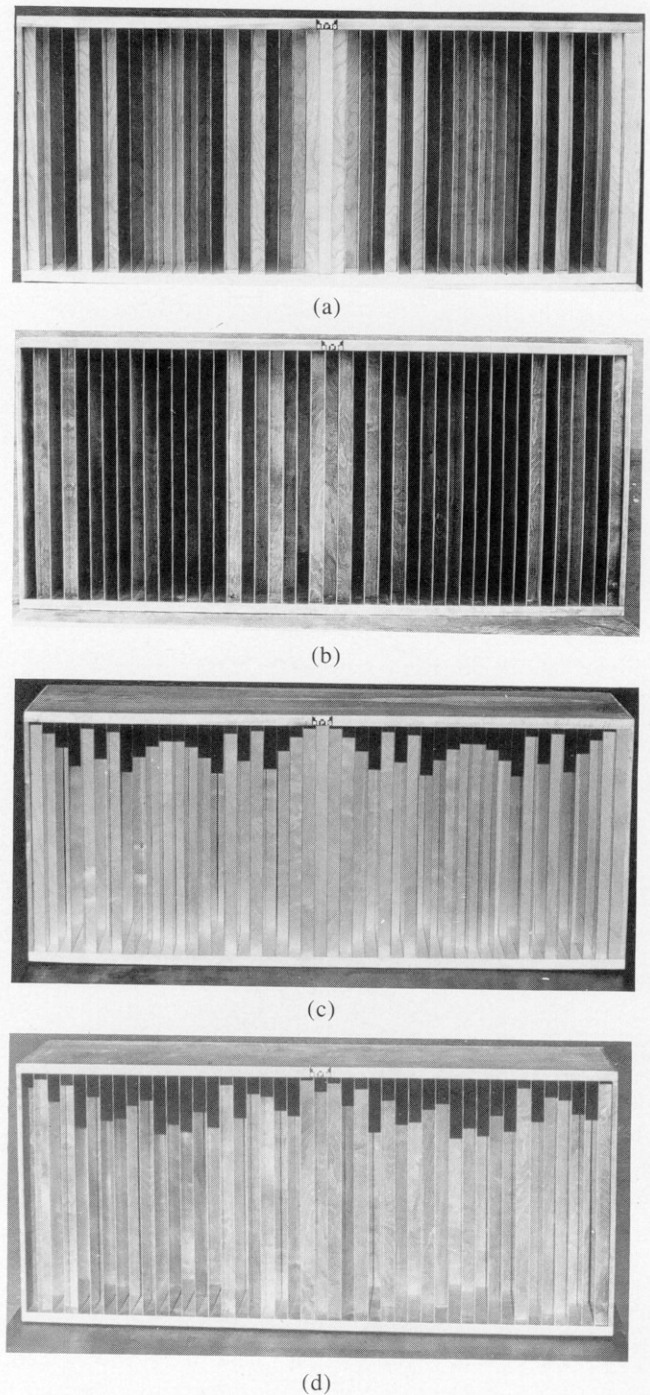


Fig. 8. Models containing two periods of a QR diffusor, with 23 wells per period [(a), (c)] and a PR diffusor, with 22 wells per period [(b), (d)], having a design bandwidth of over a decade. In (a), (c) diffuse lighting conditions were used, and in (b), (d) parallel illumination was used, so that the resulting shadows would illustrate the well depth sequences.

dersonville, Tennessee, is shown in Fig. 9. The reflection phase grating diffusors can likewise provide the necessary diffusion in a conventional live-front control room.

Many installations are in progress at the present time, as well as testing and evaluation, using the TECRON TEF³ system 10. Preliminary energy-time measurements, on the units shown in Fig. 8, were performed at the Syn-Aud-Con LEDE and Studio Design Workshop in Dallas, Texas. The experimental arrangement consisted of a Minimus 7 loudspeaker approximately 7.5 ft (2.3 m) from the diffusor being tested and an AKG 451 microphone placed 3.7 ft (1.1 m) from the diffusor surface. The loudspeaker and microphone were in a line perpendicular to the surface of the diffusor. The energy-time curve from the RPG-QR23 is shown in Fig. 10(a), the RPG-PR22 measurement is shown in Fig. 10(b), and the measurement from a flat reflective panel, placed about 4 in (0.1 m) closer to the microphone, is shown in Fig. 10(c). The energy-time curves can be roughly divided into four parts—the direct sound from loudspeaker to microphone; the reflections from the floor between loudspeaker and microphone, which in these tests were minimized with a partial treatment of absorbent material; the reflections from the diffusor; and the late arriving reflections from the surfaces of the room. The direct signal occurs at 3.4 ms and is the first intense peak in the energy-time curves. The floor reflections occur between 3.4 and 10 ms, with a peak at 7.8 ms. The reflections from the diffusors rise abruptly at 10 ms and continue for about 2 ms, in contrast with the rather sharp peak from the flat panel, in Fig. 10(c), which rises abruptly at 9.3 ms. It can be seen that the diffusor introduces substantial time spread in the diffracted wavelets compared to the flat panel. The specular peak energy from the flat panel is about 12 dB larger than either the QR or the PR diffusor peak energy, which is roughly the same.

To remove the effects of the room and isolate the diffusor reflections, the energy-time curve from the flat panel was subtracted from the diffusor measurements. The RPG-QR23 difference data are shown in Fig. 11(a) and those for the RPG-PR22 in Fig. 11(b). As mentioned earlier, the flat panel was positioned about 4 in (0.1 m) closer to the microphone to separate its reflections from those of the diffusor in the difference curves. The energy-time contour or signature, from the QR and the PR diffusor, is clearly different. The initial section of the QR pattern is the most intense part, whereas the PR curve peaks about two-thirds of the way through. These differences are due to the relative positions of the different depth wells, which are based on different sequences in the two units, with respect to the observation point. The overall time spread of about 2 ms is approximately the same for both models.

The TEF instrument can be used to evaluate the co-

herent scattering from the reflection phase grating diffusor in any direction. Such calculations and evaluations are in progress to experimentally verify performance.

The RPG program can be used to study the dynamic interference buildup, steady state, and decay, as a function of the frequency and duration of the incident sound, for the diffusors shown in Fig. 8 and a cylindrical surface with a cord length of 52.8 in (1.34 m) and a height of 14.1 in (0.27 m). The upper curves in Fig. 12 were calculated with an incident wavelength of 28.2 in (0.74 m), and the lower curves correspond to a wavelength of 7.06 in (0.18 m). All calculations were carried out with the incident and scattered waves normal to the scattering surfaces and a tone duration of 3 msec. The scattered energy is fairly independent of incident frequency in the steady state (horizontal lines) for the RPG diffusors [Fig. 12(a) and (b)]. In Fig. 12(a) the scattered energy from the QR diffusor is seen to reach a steady state after the source is on for 1.6 ms, while the PR diffusor in Fig. 12(b), having a slightly deeper maximum well depth, reaches a steady state after 1.9 ms. The unique specular cancellation property of the PR diffusor is manifested in Fig. 12(b) by the fact that the energy in the steady state is zero. A cylindrical surface, by comparison, is quite frequency dependent in the steady state [Fig. 12(c)], with the energy for the higher frequency about 4 dB down.

Many more measurements, coupled with listener preference data, in actual installations are needed to optimize fully all of the design options. The consensus of opinion, at this time, is that the reflection phase grating diffusor adds the sweetening of a concert hall to the treated room. One extremely useful consequence of treating the rear and side walls of recording control rooms with these diffusors is that a uniform stereo perspective, with no left-center and right-center voids, and spectral balance are maintained across the entire mixing console. The listener preference and accuracy

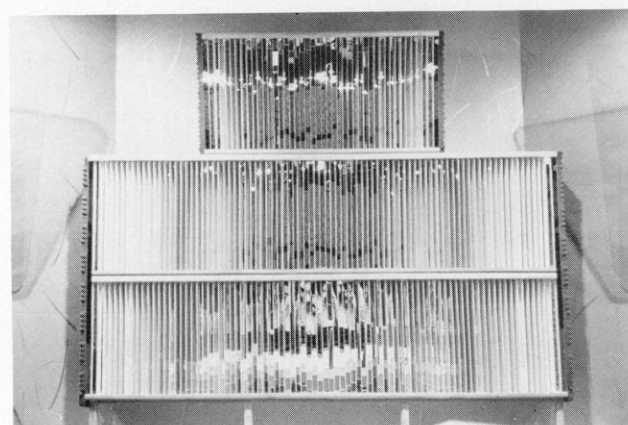


Fig. 9. Recent installation of a RPG-QR in a LEDE control room, with a bandwidth of over four octaves. In the completed project the uppermost half-size unit, along with three additional similar units, are mounted vertically (wells parallel to the floor) to diffuse incident sound in the vertical plane. The stereo perspective and spectral balance are maintained across the entire width of the mixing console when the rear wall is properly treated with the RPG diffusors.

³ TECRON and TEF are registered trademarks of TECRON, Division of Crown International.

of the stereo image are increased, because the listener is immersed in a diffuse sound field, which provides greater binaural dissimilarity or low interaural coherence [1], [3], [5]. These observations illustrate the important

binaural aspects of music perception.

Ignoring absorption, the energy reflected from a given surface area is a constant. For a flat panel, all of this energy is concentrated into specular reflection. For a one-dimensional laterally diffusing unit, with wells running vertically, for example, the energy is concentrated into a hemidisk. The thickness of the hemidisk is proportional to the projection of the well length or the height of a cluster if the diffusors are stacked as in Fig. 9. For a two-dimensional model the energy is spread into a hemisphere. The intensity in a given direction, in decibels, is approximately half as much as it would be for that same direction in the hemidisk of a one-dimensional model. Depending on how much reflected energy is needed at a given location, one can select the appropriate type of scattering surface. One-dimensional broad-band diffusors have been used on the rear and side walls in control-room applications, where imaging is important, because they can be designed to concentrate the diffuse reflections across the width of the mixing console at a desirable level with respect to the direct signal. The plane of the hemidisk can be

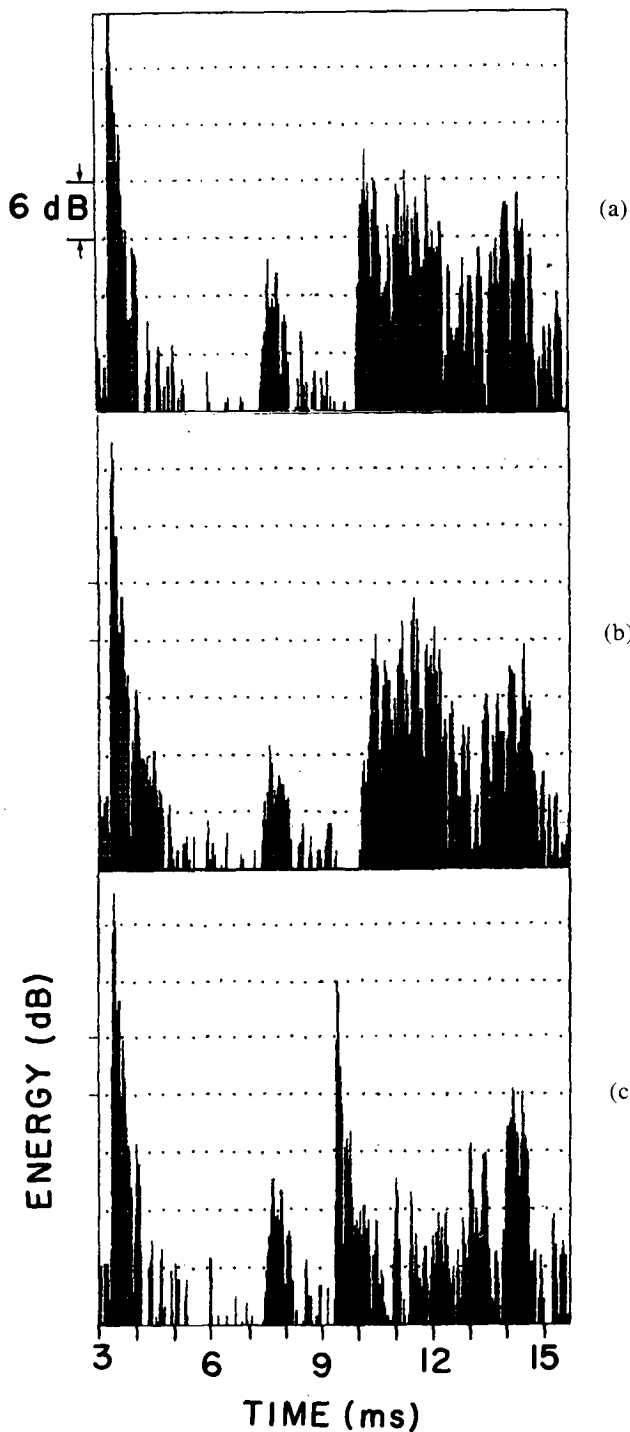


Fig. 10. Experimental energy-time curves using the TECRON TEF system 10, with a Minimus 7 loudspeaker-to-diffusor distance of 7.5 ft (2.3 m) and an AKG 451 microphone-to-diffusor distance of 3.7 ft (1.1 m), from (a) an RPG-QR23, (b) an RPG-PR22, and (c) a flat panel located 3.36 ft (1 m) from the microphone. The diffusors introduce a time spread of about 2 ms, as contrasted with the sharp specular peak of the flat panel. The base of the vertical scale is 25.3 dB referenced to 0.0002 Pascal. The line spacing is 31.77 μ s, and the line width is 43.20 μ s. The sweep rate is 7514.33 Hz/s, and the sweep range is 20.35–31 498.30 Hz. A Hamming window was used and the input configuration was balanced with 60 dB of input gain and 9 dB of IF gain.

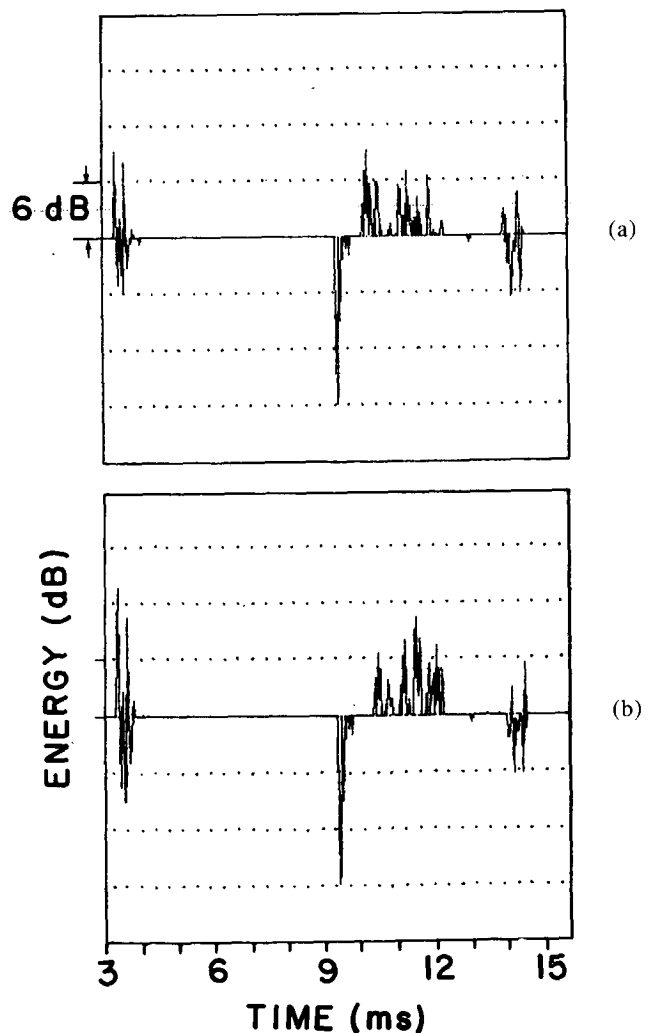


Fig. 11. To remove the effects of the room from the diffusor energy-time measurements, the energy-time curve of the flat panel, shown in Fig. 10(c), was subtracted from (a) the RPG-QR23 and (b) the RPG-PR22 measurements.

conveniently directed at the listening position by simply orienting the diffusors.

Two-dimensional designs have many near- and far-field applications, and can be used effectively to improve the acoustics of the studio. Such diffusors, with novel depth sequences, have been constructed and are being tested for performance. The symmetry of these sequences gives rise to very attractive well-depth patterns.

5 CONCLUSION

The Schroeder diffusor is a promising new approach to solving the old problem of adequate sound diffusion. Like any new concept, these reflection phase gratings must be tried and tested in a wide variety of situations to determine their usefulness. At present there are few documented installations [4], [18], in addition to those mentioned in this paper, but the number is sure to grow. Initial observations are that the diffusors provide the smoothness and sweetening of a concert hall to a treated room. Control-room monitoring has been greatly improved because the one-dimensional reflection phase grating, when properly installed, helps maintain the stereo perspective and spectral balance across the entire width of the mixing console.

To encourage application of these diffusors in critical acoustic spaces and listening environments, we have presented a review of the far-field diffraction theory; discussed relevant design parameters; provided a QR and a PR diffusor example with theoretical diffraction patterns calculated with the RPG program; and discussed a few applications, experimental measurements, and observations.

We feel that the reflection phase grating diffusor will play a key role in architectural acoustic design and look forward to being a part of this progress.

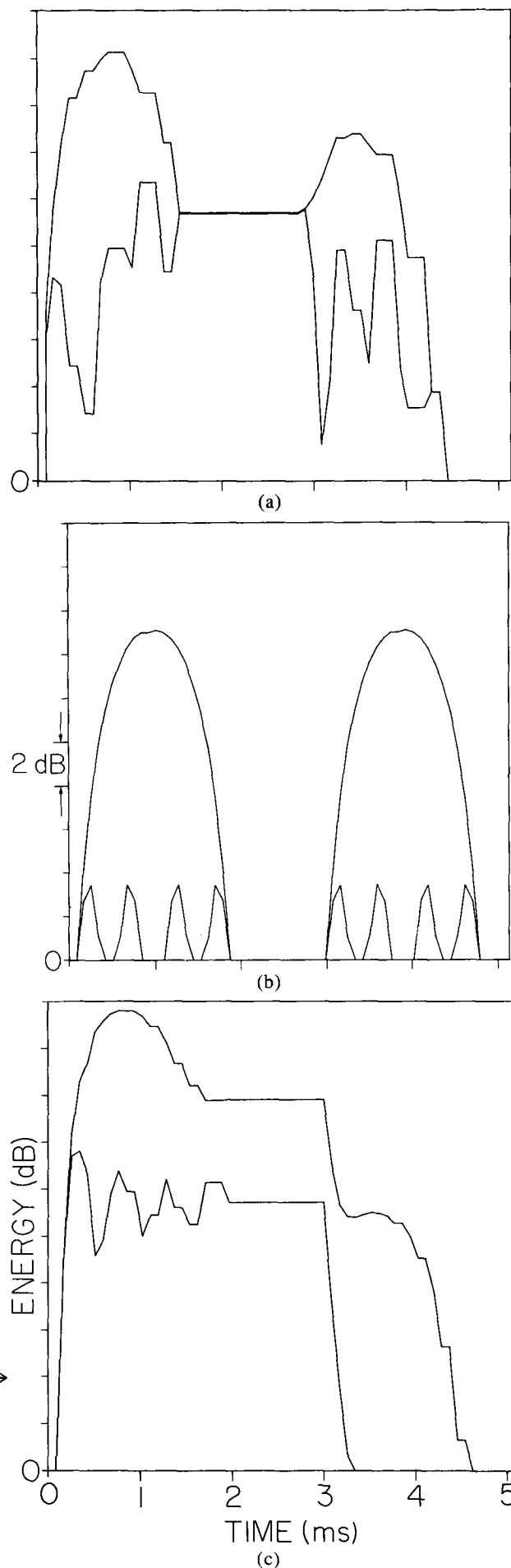
6 ACKNOWLEDGMENT

The authors wish to thank Donald M. Eger for his gracious help in obtaining the experimental energy-time curves.

7 REFERENCES

- [1] M. R. Schroeder, D. Gottlob, and K. F. Siebrasse, "Comparative Study of European Concert Halls: Correlation of Subjective Preference with Geometrical and Acoustic Parameters," *J. Acoust. Soc. Am.*, vol. 69, pp. 1195-1201 (1974).

Fig. 12. The RPG program was used to study the dynamic interference effects, as a function of the frequency and duration of the incident sound, for (a) an RPG-QR23, (b) an RPG-PR22, and (c) a cylindrical diffusor with a cord length of 43 in (1.09 m) and a height of 11.5 in (0.3 m). The upper curves are calculated for a wavelength of 23 in (0.6 m) and the lower curves correspond to a wavelength of 5.75 in (0.15 m). The interference buildup, steady state, and decay are clearly evident. It can be seen in (a), (b), that the steady-state energy for both frequencies is the same for the QR and the PR diffusors, while the cylindrical surface is frequency dependent. The calculations were carried out with the incident and scattered waves normal to the surface. The unique specular cancellation of the PR diffusor is manifested in the zero steady-state energy beginning at 1.6 ms.



[2] M. R. Schroeder, "Diffuse Sound Reflection by Maximum Length Sequences," *J. Acoust. Soc. Am.*, vol. 57, pp. 149-151 (1975).

[3] M. R. Schroeder, "Binaural Dissimilarity and Optimum Ceilings for Concert Halls: More Lateral Sound Diffusion," *J. Acoust. Soc. Am.*, vol. 65, pp. 958-963 (1979).

[4] M. R. Schroeder, "Acoustics in Human Communication: Room Acoustics, Music and Speech," *J. Acoust. Soc. Am.*, vol. 68, pp. 22-28 (1980).

[5] M. R. Schroeder, "Toward Better Acoustics for Concert Halls," *Physics Today*, vol. 33, no. 10, pp. 24-30 (1980).

[6] M. R. Schroeder, "Constant-Amplitude Antenna Arrays with Beam Patterns whose Lobes have Equal Magnitudes," *Arch. Electron. u. Übertragungstechn.*, vol. 34, p. 165 (1980).

[7] M. R. Schroeder and D. Hackman, "Iterative Calculation of Reverberation Time," *Acoustica*, vol. 45, pp. 269-273 (1980).

[8] E. N. Gilbert, "An Iterative Calculation of Auditorium Reverberation," *J. Acoust. Soc. Am.*, vol. 69, pp. 178-184 (1981).

[9] M. R. Schroeder, R. E. Gerlach, A. Steingrube, and H. W. Strube, "Response to Theory of Optimal Plane Diffusors," *J. Acoust. Soc. Am.*, vol. 65, pp. 1336-1337 (1979).

[10] A. J. Berkhout, D. W. van Wulften Palthe, and

D. de Vries, "Theory of Optimal Plane Diffusors," *J. Acoust. Soc. Am.*, vol. 65, pp. 1334-1336 (1979).

[11] H. W. Strube, "Scattering of a Plane Wave by a Schroeder Diffusor: A Mode Matching Approach," *J. Acoust. Soc. Am.*, vol. 87, pp. 453-459 (1980).

[12] H. W. Strube, "Diffraction by a Plane, Locally Reacting, Scattering Surface," *J. Acoust. Soc. Am.*, vol. 67, pp. 460-469 (1980).

[13] H. W. Strube, "More on the Diffraction Theory of Schroeder Diffusors," *J. Acoust. Soc. Am.*, vol. 70, pp. 633-635 (1981).

[14] R. C. Heyser, "Acoustical Measurements by Time Delay Spectrometry," *J. Audio Eng. Soc.*, vol. 15, pp. 370-382 (1967 Oct.).

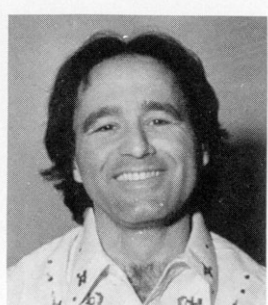
[15] R. C. Heyser, "Loudspeaker Phase Characteristics and Time Delay Distortion: Part 1," *J. Audio Eng. Soc.*, vol. 17, pp. 30-41 (1969 Jan.).

[16] R. C. Heyser, "Loudspeaker Phase Characteristics and Time Delay Distortion: Part 2," *J. Audio Eng. Soc.*, vol. 17, pp. 130-137 (1969 Apr.).

[17] D. Davis and C. Davis, "The LEDE Concept for the Control of Acoustic and Psychoacoustic Parameters in Recording Control Rooms," *J. Audio Eng. Soc.*, vol. 28, pp. 585-595 (1980 Sept.).

[18] A. H. Marshall and J. R. Hyde, "Evolution of a Concert Hall: Lateral Reflections and the Acoustical Design for Wellington Town Hall," *J. Acoust. Soc. Am.*, vol. 63, Suppl. 1, p. 536 (1978).

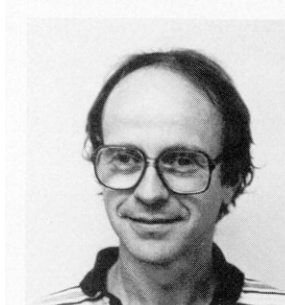
THE AUTHORS



P. D'Antonio

Peter D'Antonio was born in Brooklyn, New York, in 1941. He received a B.S. degree from St. John's University, New York, in 1963 and a Ph.D. from the Polytechnic Institute of New York in 1967. He has been employed as a research chemist at the Naval Research Laboratory, Washington, DC, since 1967, specializing in the atomic structural characterization of materials using electron, x-ray, and neutron diffraction techniques. In a private capacity, he designed and built Underground Sound Recording Studio in 1974, where he conducts acoustical research and is chief engineer. He is president of RPG Diffusor Systems, Inc., founded in 1983, to develop reflection phase grating diffusors to enhance the acoustics of critical listening environments.

Dr. D'Antonio is a member of the American Crystallographic Association, the American Chemical So-



J. Konnert

ciety, Sigma Xi, and the Audio Engineering Society.

John H. Konnert was born in Kingsville, Ohio, in 1941. He received a B.A. degree from the College of Wooster in 1963 and a Ph.D. from the University of Minnesota in 1967. He has been employed as a research chemist at the Naval Research Laboratory, Washington, DC, since 1967 and has developed many techniques for obtaining detailed atomic structural information from electron, x-ray, and neutron diffraction data. At present he is involved with micro- and nanodiffraction using electron microscopy. He is a founding member and vice president of RPG Diffusor Systems, Inc.

Dr. Konnert is a member of the American Crystallographic Association, the American Chemical Society, and Sigma Xi.